Article

Critical Assessment of Information Back-Flow in Measurement-Free Teleportation

Hannah McAleese [1,*] and Mauro Paternostro [1,2]

1   Centre for Quantum Materials and Technologies, School of Mathematics and Physics, Queen's University Belfast, Belfast BT7 1NN, UK
2   Department of Physics and Chemistry-Emilio Segrè, University of Palermo, Via Archirafi 36, I-90123 Palermo, Italy
*   Correspondence: h.mcaleese@qub.ac.uk

Abstract: We assess a scheme for measurement-free quantum teleportation from the perspective of the resources underpinning its performance. In particular, we focus on claims recently made about the crucial role played by the degree of non-Markovianity of the dynamics of the information carrier whose state we aim to teleport. We prove that any link between the efficiency of teleportation and the back-flow of information depends fundamentally on the way the various operations entailed by the measurement-free teleportation protocol are implemented while—in general—no claim of causal link can be made. Our result reinforces the need for the explicit assessment of the underlying physical platform when assessing the performance and resources for a given quantum protocol and the need for a rigorous quantum resource theory of non-Markovianity.

Keywords: open-system dynamics; non-Markovianity; quantum resources

1. Introduction

Quantum teleportation [1] shows the power of entanglement as a resource: by jointly measuring the quantum states of two particles, we can transfer, without any actual exchange of matter, a quantum state to a remote station. This process is commonly referenced in the context of quantum communication over long distances, but its applications to quantum computation are also paramount, as demonstrated by the success of the measurement-based model for quantum computing [2]. The measurement-free teleportation protocol, put forward in Ref. [3], helped illustrate the centrality of entanglement by entirely removing measurements that, in contrast, are very important for the success of the original scheme [1].

Ref. [4] challenged the nearly dogmatic view on the essential role of entanglement to explore the relation between the efficiency of measurement-free teleportation and non-Markovianity [5–7]. Specifically, the analysis by Tserkis et al. drew links between the information back-flow from the *instrumental part* of the computational register (considered to be an environment) to its *relevant part* (the system), and the entanglement present in the environment. It is worth noticing that the original teleportation protocol has previously been studied in the context of non-Markovianity [8–11], but such an assessment has normally been done by introducing an external environment. A different take to the *role* played by non-Markovianity in teleportation was addressed in Ref. [8], where non-Markovianity was seen as an additive to performance rather than the mechanism underpinning it. Ref. [11], instead, studied the use of non-Markovianity to mitigate against the effects of noise on the resource state.

This paper arises from the work of Tserkis [4] and critically assesses the link between non-Markovianity and efficiency in the measurement-free teleportation protocol. Methodologically, we model the teleportation circuit *as a quantum channel* for a system of interest [12–17] and analyze the dynamics inherent within it.

While we do not introduce non-Markovianity through any external means, by focusing on the measurement-free teleportation approach, we are able to gain insight into the underlying dynamics of teleportation and analyze the non-Markovianity which could be inherently present in the protocol.

We show that such connections are—at best—very weak and delicately dependent on the way the dynamics underpinning the protocol are implemented and interpreted. Only a very fine-grained assessment of the various stages of the teleportation channel allows us to unveil how non-Markovianity enters the dynamics of the register and, potentially, could play a role in the establishment of the right fluxes of information from the instrumental part of the teleportation register to its relevant part. On the one hand, our results point towards the careful assessment of the way a dynamical map is implemented in all its sub-parts before any conclusions on what embodies a *resource* of it can be made. On the other hand, it indirectly points to the need for a deeper understanding of the role played by non-Markovianity in quantum information problems and, in turn, the benefits of developing a comprehensive quantum resource theory of non-Markovianity [18,19].

The remainder of this paper is organized as follows: in Section 2, we illustrate the measurement-free teleportation protocol and address it from the perspective of open-system dynamics, including the effects of its *channel description* on distinguishability of input states. Section 3 reviews the key instruments for our quantitative assessment of non-Markovianity and applies them to the evaluation of the information back-flow entailed by the measurement-free teleportation protocol. Section 4 assesses in detail the link with quantum correlations shared by the relevant and ancillary part of the register, highlighting the controversial nature of claims linking such physical quantities and the performance of the scheme itself. Finally, Section 5 offers our conclusions and perspectives.

2. Measurement-Free Teleportation

We follow the three-qubit measurement-free teleportation protocol put forward in Ref. [3], whose quantum circuit we present in Figure 1. As our aim is to study the information back-flow and non-Markovianity in the protocol itself, it is appropriate to use the language of open quantum systems when describing it. We thus use the label S for the *system* whose state is being teleported, and $E_{1,2}$ for the *environmental* particles that are ancillary for the protocol.
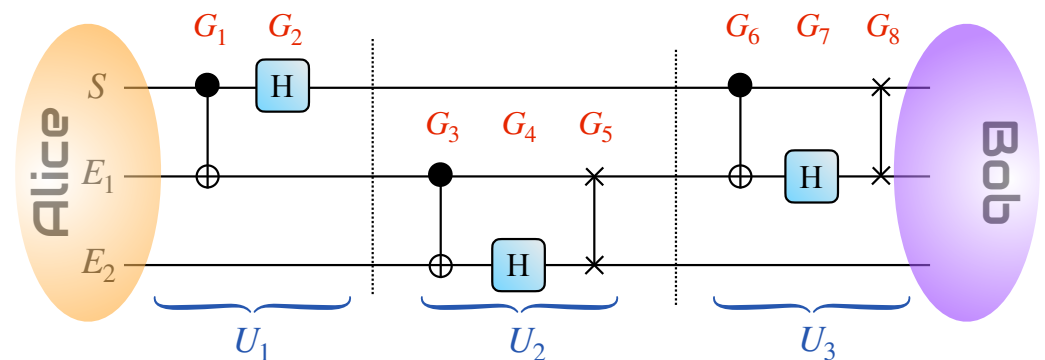

Figure 1. Quantum circuit of the measurement-free teleportation protocol. Each gate into which the circuit is decomposed is labeled as G_i ($i \in \{1, \dots, 8\}$). They can be grouped into three unitary *blocks* of operations U_j ($j = 1, 2, 3$) as defined in Equations (2)–(5). Here, $G_{1,3,6}$ are CNOT gates, $G_{2,4,7}$ are Hadamard transforms, while $G_{5,8}$ are SWAP gates.

Two agents, conventionally identified as Alice and Bob, hold control of the full register consisting of system and environment as per Figure 1. Alice aims to teleport to Bob the state $|\psi(\alpha)\rangle = \alpha|0\rangle + \sqrt{1 - |\alpha|^2}|1\rangle$, which she encodes in qubit S. On the other hand, qubits $E_{1,2}$ make up a resource state.

In the original formulation of the measurement-free protocol in Ref. [3], the teleported state was encoded in the degrees of freedom of one of the environmental qubits (specifically,

E_2). The authors of Ref. [4] proposed an altered version of the scheme where $|\psi\rangle$ is recovered from qubit S. This, as mentioned before, put them in a position to argue for a direct relationship between the quality of retrieval of $|\psi\rangle$ from the degrees of freedom of S and the non-Markovian character of the system-environment dynamics. As our scope is to critically assess the actual implications of non-Markovianity for the effectiveness of the protocol, we will adhere to the formulation in Ref. [4]. We emphasize that, though this modification is beneficial for studying and understanding the underlying dynamics, we would use the original formulation in Ref. [3] to teleport states in a quantum computation context.

In an ideal teleportation scheme, the resource encoded in the E_1-E_2 compound would be a maximally entangled Bell state. Here, to study the necessary correlations for the protocol at hand, we weaken this strong requirement and take the resource to be the Werner state

$$W_{E_1 E_2}(p) = p|\phi^+\rangle\langle\phi^+|_{E_1 E_2} + \frac{1-p}{4}\mathbb{1}_{E_1 E_2}, \tag{1}$$

where $p \in [0,1]$ and $|\phi^+\rangle_{E_1 E_2} = (|00\rangle + |11\rangle)_{E_1 E_2}/\sqrt{2}$ is a Bell state. Unless $p = 0$, there are correlations present in $W_{E_1 E_2}(p)$: it is entangled for $p \in (1/3, 1]$ and carries quantum discord and classical correlations for $0 < p \leq 1$.

Alice sends S and E_1 through the circuit to Bob. The operations $G_j(j = 1, ..., 8)$ undergone by the S-E_1 compound can be grouped into three *blocks* to highlight their roles in the process. The first is

$$U_1 = (H_S \otimes \mathbb{1}_{E_1 E_2})(\text{CNOT}_{SE_1} \otimes \mathbb{1}_{E_2}). \tag{2}$$

Here $H = (X + Z)/\sqrt{2}$ stands for the Hadamard gate and $\text{CNOT}_{SE_1} = |0\rangle\langle0|_S \otimes \mathbb{1}_{E_1} + |1\rangle\langle1|_S \otimes X_{E_1}$ is a controlled-NOT gate (with X and Z the Pauli x and z matrix, respectively). Owing to the interaction entailed by such a gate, quantum correlations might be established between S and E_1 through the action of U_1. At this point, at least some of the information about the system state is encoded in the form of system-environment correlations. The degree to which this happens, though, depends on the initial state of the system: for $\alpha = 0$, S and the environment remain uncorrelated, while the total correlations are maximized for $\alpha = 1/\sqrt{2}$. At this stage, due to the initial correlations within the environment, all elements of the register would be quantum correlated, in general.

The second block takes the form of the unitary gate

$$U_2 = (\mathbb{1}_S \otimes \text{SWAP}_{E_1 E_2})(\mathbb{1}_{SE_1} \otimes H_{E_2})(\mathbb{1}_S \otimes \text{CNOT}_{E_1 E_2}) \tag{3}$$

with $\text{SWAP}_{E_1 E_2}$ the swap gate which, for any state $|\phi\rangle_{E_1}|\eta\rangle_{E_2}$, acts as

$$\text{SWAP}_{E_1 E_2}|\phi\rangle_{E_1}|\eta\rangle_{E_2} = |\eta\rangle_{E_1}|\phi\rangle_{E_2}. \tag{4}$$

In the ideal case where the environment is initially maximally entangled (i.e., for $p = 1$), the U_2 operation acts to decouple S and E_2, therefore localizing the information encoded through U_1 between S and E_1 only. Some correlations do remain between all three systems for $p < 1$.

The final block of unitaries of the protocol is

$$U_3 = (\text{SWAP}_{SE_1} \otimes \mathbb{1}_{E_2})(\mathbb{1}_S \otimes H_{E_1} \otimes \mathbb{1}_{E_2})(\text{CNOT}_{SE_1} \otimes \mathbb{1}_{E_2}). \tag{5}$$

2.1. Effective Depolarizing-Channel Description

In the original protocol with $p = 1$ [3], all system-environment correlations vanish after the application of U_3, and all the information about the input state is localized in the desired system. In the version discussed here, with an imperfect resource, the success of the protocol grows with p.

To see this quantitatively, we resort to an effective description of the dynamics undergone by system S as a result of the action of the quantum circuit and its coupling to the

environmental qubits. We call $\rho_S^i = |\psi\rangle\langle\psi|_S$ the initial state of the system qubit, label as $\mathcal{U} = U_3 U_2 U_1$ the total unitary of the circuit and decompose the identity $\mathbf{1}_{E_1 E_2}$ in the Hilbert space of the environmental compound over the Bell basis $\{|\mathcal{B}_j^\alpha\rangle\}_{E_1 E_2} \equiv \{|\phi^\pm\rangle, |\psi^\pm\rangle\}_{E_1 E_2}$, where $\alpha = \phi, \psi$ and $j = \pm$ and we introduce the remaining Bell states

$$|\phi^-\rangle_{E_1 E_2} = \frac{1}{\sqrt{2}}(|00\rangle - |11\rangle)_{E_1 E_2},$$
$$|\psi^\pm\rangle_{E_1 E_2} = \frac{1}{\sqrt{2}}(|01\rangle \pm |10\rangle)_{E_1 E_2}. \tag{6}$$

The final state of S thus reads

$$\rho_S^f = \mathrm{Tr}_{E_1 E_2}\left[\mathcal{U}\left(\rho_S^i \otimes W_{E_1 E_2}(p)\right)\mathcal{U}^\dagger\right]. \tag{7}$$

Upon inserting Equation (1) into this expression, we have

$$
\begin{aligned}
\rho_S^f &= p \sum_{j,k=0,1} {}_{E_1 E_2}\langle jk|\mathcal{U}|\phi^+\rangle_{E_1 E_2}\rho_S^i {}_{E_1 E_2}\langle \phi^+|\mathcal{U}^\dagger|jk\rangle_{E_1 E_2} \\
&+ \frac{1-p}{4}\sum_{j,k,\alpha,l} {}_{E_1 E_2}\langle jk|\mathcal{U}|\mathcal{B}_l^\alpha\rangle_{E_1 E_2}\rho_S^i {}_{E_1 E_2}\langle \mathcal{B}_l^\alpha|\mathcal{U}^\dagger|jk\rangle_{E_1 E_2} \\
&= \frac{1+3p}{4}\sum_{j,k=0,1} \mathcal{V}_{jk}^{\phi^+}\rho_S^i \mathcal{V}_{jk}^{\phi^+ \dagger} + \frac{1-p}{4}\sideset{}{'}\sum_{j,k,\alpha,l} \mathcal{V}_{jk}^{\alpha l}\rho_S^i \mathcal{V}_{jk}^{\alpha l \dagger},
\end{aligned} \tag{8}
$$

where the symbol $\sum_{\alpha,l}'$ stands for the summation over all the elements of the Bell basis except $|\phi^+\rangle_{E_1 E_2}$ and we have introduced the operators $\mathcal{V}_{jk}^{\alpha l} = {}_{E_1 E_2}\langle jk|\mathcal{U}|\mathcal{B}_l^\alpha\rangle_{E_1 E_2}$ of the open-system dynamics undergone by S. An explicit calculation leads to the results summarized in Table 1.

Table 1. Summary of the explicit form taken by the operators $\mathcal{V}_{jk}^{\alpha l}$ acting in the Hilbert space of S [cf. Equation (8)].

$\mathcal{V}_{jk}^{\alpha l}$	$j=0, k=0$	$j=0, k=1$	$j=1, k=0$	$j=1, k=1$
$\mathcal{V}_{jk}^{\phi^+}$	$\mathbf{1}_S/2$	$\mathbf{1}_S/2$	$\mathbf{1}_S/2$	$\mathbf{1}_S/2$
$\mathcal{V}_{jk}^{\phi^-}$	$Z_S/2$	$-Z_S/2$	$Z_S/2$	$-Z_S/2$
$\mathcal{V}_{jk}^{\psi^+}$	$X_S/2$	$X_S/2$	$-X_S/2$	$-X_S/2$
$\mathcal{V}_{jk}^{\psi^-}$	$-iY_S/2$	$iY_S/2$	$iY_S/2$	$-iY_S/2$

Using such expressions, we are finally able to recast the final state of the system in the form of the operator-sum decomposition $\rho_S^f = \sum_{j=1}^4 \mathcal{K}_j \rho_S^i \mathcal{K}_j^\dagger$ with

$$
\mathcal{K}_1 = \sqrt{\frac{1+3p}{4}}\mathbf{1}_S, \quad \mathcal{K}_2 = \sqrt{\frac{1-p}{4}}Z_S,
$$
$$
\mathcal{K}_3 = \sqrt{\frac{1-p}{4}}X_S, \quad \mathcal{K}_4 = \sqrt{\frac{1-p}{4}}Y_S, \tag{9}
$$

which immediately gives $\sum_{j=1}^4 \mathcal{K}_j^\dagger \mathcal{K}_j = \mathbf{1}_S$ and allows us to conclude that the action of the measurement-free teleportation protocol on the state of the system is that of a depolarizing channel acting with a resource-dependent rate $q = 1 - p$. The corresponding state fidelity with ρ_S^i reads

$$F(p) = {}_S\langle\psi|\rho_S^f|\psi\rangle_S = (1+p)/2, \tag{10}$$

thus increasing linearly from $1/2$ when $p = 0$, to 1 when $p = 1$. The role of the SWAP_{SE_1} gate in U_3 is to transfer the information on $|\psi\rangle$ otherwise encoded in the state of E_1 to the system qubit S. As already anticipated, the inclusion of this gate in the protocol allows us to characterize the quality of the teleportation performance in terms of state-revival in the system qubit.

2.2. Distinguishability and Non-Markovianity Resulting from the Dynamics

While this analysis shows the non-trivial nature of the overall action of the quantum circuit on the state of S, it is instructive to dissect the effects of the individual U_j, particularly in terms of the degree of distinguishability of different input states of S. To do this quantitatively, we make use of the instrument embodied by the trace distance between two quantum states. This is defined as

$$D(\rho_1, \rho_2) = \frac{1}{2}\|\rho_1 - \rho_2\|_1, \tag{11}$$

where $\rho_{1,2}$ are two arbitrary density matrices and $\|A\|_1 = \text{Tr}[\sqrt{A^\dagger A}]$ is the trace norm of an arbitrary matrix A.

First, let us consider the action of U_1 on the initial state of S. Following an approach fully in line with the one formalized in Equation (8) but for $\mathcal{U} \to U_1$ and by labeling the state of S resulting from the application of this block of unitaries alone as $\rho_S^1(\alpha)$, so as to emphasize the dependence on the initial-state parameter α, we have

$$\rho_S^1(\alpha) = \sum_{i=1,2} K_i \rho_S^i K_i^\dagger = \alpha^2 |+\rangle\langle+|_S + (1 - \alpha^2)|-\rangle\langle-|_S, \tag{12}$$

where we have introduced the Kraus operators $K_1 = |+\rangle\langle 0|_S$ and $K_1 = |-\rangle\langle 1|_S$, which are written in terms of the eigenstates $|\pm\rangle_S$ of X_S such that $X_S|\pm\rangle_S = \pm|\pm\rangle_S$. We thus consider

$$D(\rho_S^1(\alpha_1), \rho_S^1(\alpha_2)) = |\alpha_1^2 - \alpha_2^2|, \tag{13}$$

where $\alpha_{1,2} \in \mathbb{R}$ (without loss of generality) identifies two different initial states of the system. Having in mind the analysis of the degree of non-Markovianity that will be presented later in this work, we take $\alpha_1 = 1$ and $\alpha_2 = 0$ (so as to prepare S in eigenstates of Z_S) and thus consider fully distinguishable input states. For such a choice, we have $D(\rho_S^1(\alpha_1), \rho_S^1(\alpha_2)) = 1$, achieving again full distinguishability regardless of the properties of the environmental system (as $\rho_S^1(\alpha)$ does not depend on p).

As for U_2, it is clear from Figure 1 that this block of unitaries is *local* with respect to the bipartition S-$(E_1 E_2)$, i.e., U_2 does not contain degrees of freedom of S, which implies that the corresponding operator-sum decomposition of the effective channel acting on the system involves only the identity operator $\mathbb{1}_S$. The evolved state ρ_S^2 after U_2 is thus identical to Equation (12). Notice, though, that the state of the environment will be changed by this part of the circuit.

Finally, block U_3 will need to be applied to the—in general quantum correlated— joint state of S-$(E_1 E_2)$. This immediately gives evidence of the fundamental difference between the action entailed by U_3 and the other blocks of operations: while, as for U_1, this operation couples S to the environment, the input state to U_3 is a state that features, as mentioned above, system-environment correlations that *may* play a key role in determining the nature of the dynamics of S. Technically, such correlations prevent us from using the same approach as above to identify the effective channel acting on S. Instead, we will have to calculate

$$\rho_S^3 \equiv \rho_S^f = \Phi_p(\rho_S^i) = \text{Tr}_{E_1 E_2}\left[U_3 \rho_{S E_1 E_2}^2 U_3^\dagger\right]$$

$$= \frac{1}{2}\begin{pmatrix} 2\alpha^2 p - p + 1 & 2\alpha\sqrt{1-\alpha^2}p \\ 2\alpha\sqrt{1-\alpha^2}p & -2\alpha^2 p + p + 1 \end{pmatrix} \tag{14}$$

with $\rho_{\tilde{S}E_1E_2}^2$ the output state of the system-environment compound after application of U_2U_1, and $\Phi_p(\cdot)$ the p-dependent dynamical map resulting from taking the trace over the environmental degrees of freedom. The trace distance between two input states of S reads

$$
\begin{aligned}
D(\rho_S^f(\alpha_1), \rho_f^1(\alpha_2)) &= p\left| \alpha_1\sqrt{1-\alpha_2^2} - \alpha_2\sqrt{1-\alpha_1^2} \right| \\
&= pD(|\psi(\alpha_1)\rangle\langle\psi(\alpha_1)|_S, |\psi(\alpha_2)\rangle\langle\psi(\alpha_2)|_S).
\end{aligned}
\tag{15}
$$

This shows that the last block of the quantum circuit at hand is the only one that could change the degree of distinguishability between the input state and the evolved one, which, in general, shrinks linearly with the depolarization rate.

3. Analysis of Non-Markovianity in the Measurement-Free Teleportation Circuit

We are now able to leverage the tools and results achieved so far to assess the non-Markovian features of the dynamics entailed by the measurement-free teleportation protocol. We start by briefly reviewing some of the most popular measures of non-Markovianity reported so far in the literature.

3.1. Review of Measures of Non-Markovianity

In this short review, we do not aim to be comprehensive and refer the interested reader to Refs. [5–7].

3.1.1. Breuer–Laine–Piilo Measure

The measure of non-Markovianity, which we will rely on the most, is the one proposed by Breuer, Laine, and Piilo (BLP) in Ref. [20]. It builds on the fact that the trace distance decreases monotonically under Markovian dynamics, any increase signaling non-Markovianity.

The measure is, therefore, calculated as

$$
\mathcal{N}_{BLP} = \max_{\rho_{1,2}(0)} \int_{\sigma>0} \sigma(t, \rho_{1,2}(0)) \, dt,
\tag{16}
$$

where $\sigma(t, \rho_{1,2}(0)) = \partial_t D(\rho_1(t), \rho_2(t))$ is the rate of change of the trace distance between two initial states $\rho_{1,2}(0)$ of the systems we are hoping to distinguish, considered over all the time intervals (a_i, b_i) where $\sigma > 0$ (i.e., where the trace distance increases). This can alternatively be expressed in a simpler form as

$$
\mathcal{N}_{BLP} = \max_{\rho_{1,2}(0)} \sum_i [D(\rho_1(b_i), \rho_2(b_i)) - D(\rho_1(a_i), \rho_2(a_i))].
\tag{17}
$$

Please note that growth in trace distance is a necessary but not sufficient condition for non-Markovianity. We, therefore, include other measures in this paper to ensure that we are not missing non-Markovian dynamics in the protocol even when $\mathcal{N}_{BLP} = 0$.

We can simplify the optimization procedure using the result that optimal initial-state pairs will be antipodal points on the surface of the Bloch sphere [21].

3.1.2. Rivas-Huelga-Plenio Measure

The Rivas-Huelga-Plenio (RHP) measure [22], on the other hand, is based on a necessary and sufficient condition for Markovianity. A dynamical map between two times $t + \epsilon$ and t where $t > 0$ can be written as

$$
\mathcal{E}_{(t+\epsilon,t)} = \mathcal{E}_{(t+\epsilon,0)}\mathcal{E}_{(t,0)}^{-1},
\tag{18}
$$

where the inverse map $\mathcal{E}_{(t,0)}^{-1}$ may not be completely positive. Given a maximally entangled state of the system and an ancilla, such as $|\phi^+\rangle_{SA}$, we apply the dynamical map $\mathcal{E}_{(t+\epsilon,t)} \otimes \mathbf{1}$. The dynamics are Markovian if and only if $f_{NCP} = 1$ where

$$f_{NCP}(t+\epsilon, t) = \|(\mathcal{E}_{(t+\epsilon,t)} \otimes \mathbf{1})|\phi^+\rangle\langle\phi^+|\|_1, \tag{19}$$

which can be recast as $g(t) = 0$ with

$$g(t) = \lim_{\epsilon \to 0^+} \frac{f_{NCP}(t+\epsilon, t) - 1}{\epsilon}. \tag{20}$$

The corresponding measure of non-Markovianity is then

$$\mathcal{N}_{RHP} = \int_0^\infty g(t)\, dt. \tag{21}$$

The quantity measure $\mathcal{N}_{RHP}/2$ is a lower bound of the robustness of non-Markovianity [19]. We can, therefore, attribute a physical meaning to it, i.e., the amount of noise that must be added to a non-Markovian operation before it becomes Markovian.

3.1.3. Luo-Fu-Song Measure

The correlations-based measure proposed by Luo, Fu, and Song (LFS) in Ref. [23] follows a similar reasoning as the BLP one. The quantum mutual information between a system and an ancilla $I(\rho_{SA})$, which can be calculated as

$$I(\rho_{SA}) = S(\rho_S) + S(\rho_A) - S(\rho_{SA}), \tag{22}$$

where $S(\rho) = -\text{Tr}(\rho \log_2 \rho)$ is the von Neumann entropy of state ρ, is monotonically decreasing under Markovian dynamics acting on the system only. Therefore, any increase in mutual information witnesses non-Markovianity.

We write the rate of change in the mutual information as $\gamma(\rho_{SA}(t)) = \partial_t I(\rho_{SA}(t))$ with $\rho_{SA}(t) = (\Phi_S \otimes \mathbf{1}_A)\rho_{SA}(0)$. The measured building on this rate is therefore given by

$$\mathcal{N}_{LFS} = \int_{\gamma>0} \gamma(\rho_{SA}(t))\, dt, \tag{23}$$

where the integral is taken, once more, in the regions where $\gamma > 0$. In line with the Choi-Jamiołkowski isomorphism, we take the initial state $\rho_{SA}(0)$ to be any maximally entangled state to evaluate the measure.

3.2. Information Back-Flow and Non-Markovianity

We begin by taking a straightforward approach to the description of the generator of the dynamical map. We provide an effective Hamiltonian of the system and environment by considering

$$H_{\text{eff}} = -i \ln \mathcal{U}, \tag{24}$$

where we have assumed units such that $\hbar = 1$. Fixing a branch for the logarithm makes it single-valued and H uniquely determined from $\mathcal{U}$. The inspection of H_{eff}, which we do not report here as too complex, reveals that—in general—such a Hamiltonian involves three-body interactions between S, E_1 and E_2.

Considering the corresponding time-evolution operator $e^{-iH_{\text{eff}}t}$ and varying the parameter p, we evaluate each of the measures reviewed in Section 3.1. The results are plotted in Figure 2. The degree of non-Markovianity of the dynamics of S remains small for each of the measures and is virtually negligible for states of the environment with $p \lesssim 0.7$. However, as expected, the RHP measure is the most sensitive and detects non-Markovianity within a larger range of values of the mixing parameter in Equation (1): the lowest value witnessing non-Markovianity through RHP is $p = 0.41$, to be compared to $p = 0.5$ for BLP

and $p = 0.65$ for LFS. As Werner states are inseparable for $p > 1/3$; the environment is always entangled when the dynamics are non-Markovian.
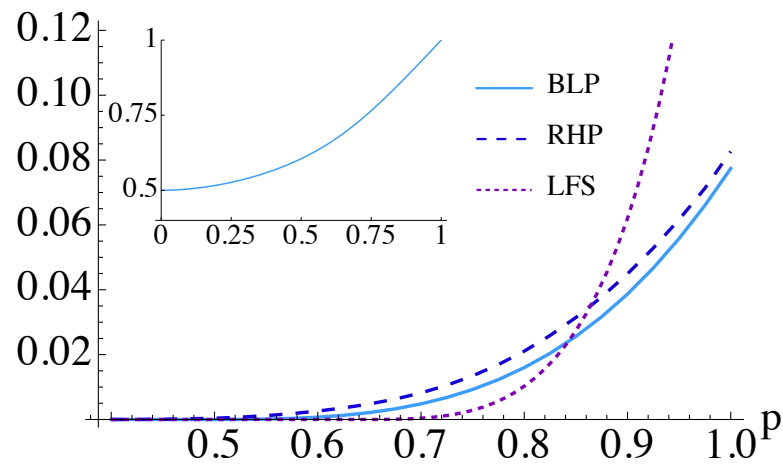

Figure 2. Non-Markovianity of the dynamics given by Equation (24). Results are plotted only for $p \geq 0.4$ as all the measures listed in Section 3.1 are zero for $0 \leq p \leq 0.4$. Inset: Non-Markovianity of the effective Hamiltonian in Equation (25) as measured by the $\mathcal{N}_{BLP}$ measure.

We can, however, take a different approach to the dynamics. Instead of working *block by block*, we use a fine-grained approach that considers each G_j gate in sequence [cf. Figure 1]. We thus address the eight effective Hamiltonian operators

$$H_{\text{eff},j} = -i \log G_j \quad (j = 1, ..., 8) \tag{25}$$

and use the corresponding time-evolution operators to describe the dynamics. This assumption results in dramatically different values of the BLP measure, which are displayed in Figure 2, thus proving that the unitary block-based approach was too coarse-grained to gather the features of the circuit dynamics. Surprisingly, in this case, we find non-Markovianity even when the environment is prepared in a maximally mixed state (i.e., for $p = 0$). The BLP measure gives much larger values in this case compared to the previous modeling. While the initial states of S that should be used in the calculation of the BLP measure in the block-based approach are the eigenstates of Z_S, in the individual gate-based model, such states change depending on p.

What is the physical origin of the non-null degree of non-Markovianity for $p = 0$? In Figure 3, we plot the trace distance when $p = 0$ and we begin with $|0\rangle$ and $|1\rangle$ in S (the optimal states when the environment is completely uncorrelated). We see that the trace distance increases only during the last gate, a SWAP operation between S and E_1. This is true even when we change the initial state of the system. We remark that this gate is not in the original measurement-free teleportation circuit but was added in Ref. [4] to consider the impact of the protocol on one single system. The original circuit starts with the same gates G_1–G_4 as in Figure 1, followed by a CNOT between S and E_2 and a Hadamard gate acting on E_2 [3]. The initial system state $|\psi\rangle$ is therefore teleported to E_2 without returning to S. If we revert to the original protocol and consider the dynamics of E_2, tracing out S and E_1, we can see if there is any increase in trace distance. This is similar to the method used in Ref. [12], for example. We have plotted the results in Figure 4.

We find that the trace distance remains zero for $p = 0$ but does grow for $p > 0$. In fact, in terms of the BLP measure, we find that $\mathcal{N}_{BLP} = p$. Therefore, only for $p = 0$ can we claim that the non-Markovianity comes merely from the extra SWAP gate. Though the results in Figure 4 are limited to the initial state pair $\{|0\rangle, |1\rangle\}$, we find that there is no increase in trace distance for any alternative initial states. However, for $p > 0$, we can see that trace distance does indeed increase, and non-Markovianity is therefore present even when we label E_2 as our "system" instead of S.
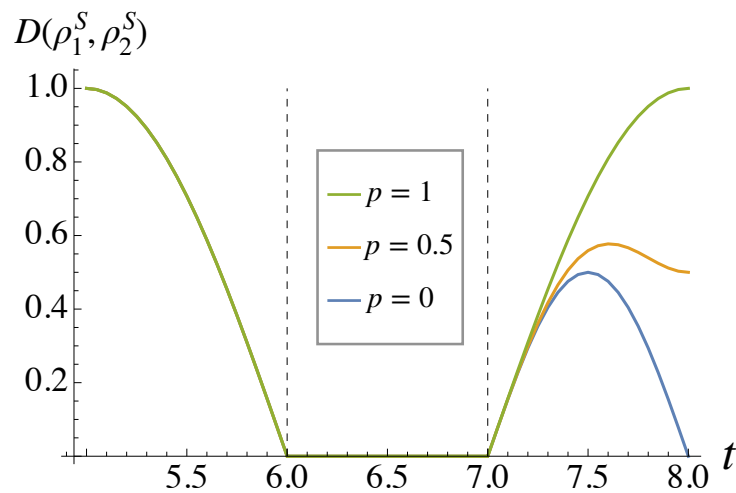
Figure 3. Trace distance between the two states of S as they go through the teleportation circuit. Gate G_i acts when $i - 1 < t < i$. We plot only $5 \le t \le 8$ as the trace distance remains constant at 1 for $t < 5$.
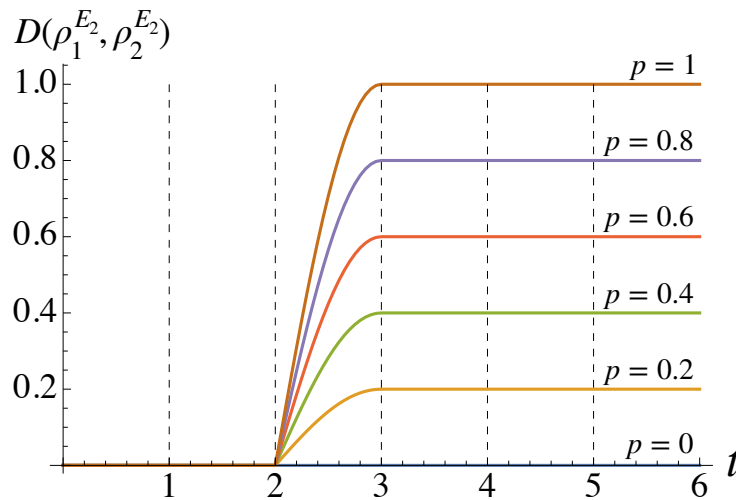

Figure 4. Trace distance between the two states of E_2 for the original BBC protocol [3] as time evolves. The dashed lines are boundaries between the gates acting on the system and the environment. Gates G_1–G_4 correspond to those in Figure 1, while G_5 is a CNOT operation on SE_2 and G_6 is a Hadamard gate on E_2.

4. Information Back-Flow and Correlations

In the previous section, we discovered that the relation between non-Markovianity, the performance of the teleportation scheme, and the entanglement in the initial state of the environment depends on whether the implementation of the circuit allows for the consideration of the individual G_j gates rather than the blocks of unitaries playing key roles in the evolution of the state of S. In the latter arrangement, the dynamics of S is non-Markovian for $p \geq 0.41$; in the former, non-Markovianity is present in the map evolving S even when the environment is in a separable state, thus breaking the connection established in Ref. [4]. We now study the relation between non-Markovianity of the dynamics and system-environment correlations as time evolves.

Initially, correlations are only present in the environmental Werner state. As done previously, we begin by describing the dynamics using the Hamiltonian in Equation (24). Figure 5a displays the entanglement between the system and environment as time evolves from an input state of $|\psi\rangle_S = |0\rangle$, as measured by the logarithmic negativity [24,25]

$$E = \log_2 \|\rho_{SE_1E_2}^{T_S}\|_1 \tag{26}$$

to quantify the entanglement in the bipartition S-vs-$(E_1 E_2)$, where $\rho_{SE_1 E_2}^{T_S}$ is the partial transpose of the evolved state S-$(E_1 E_2)$ compound with respect to S. As might have been expected, the larger the initial environmental entanglement (as related to p), the more entanglement is shared between S and $(E_1 E_2)$ during the protocol, and this corresponds to a larger degree of non-Markovianity.
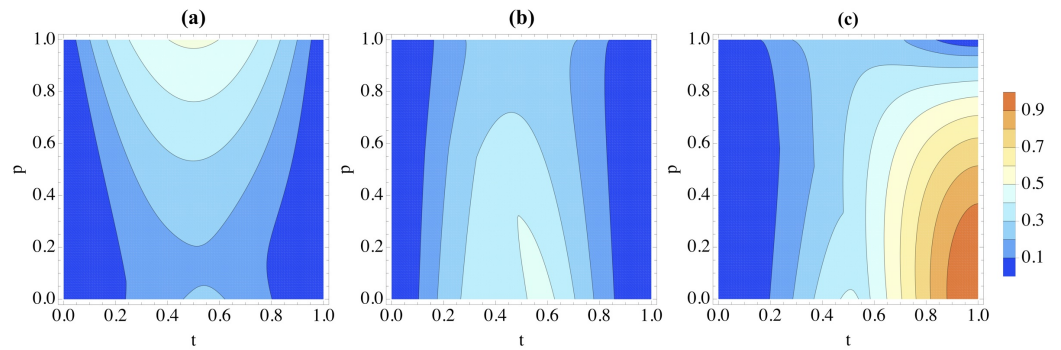

Figure 5. Correlations in the splitting S-vs-$(E_1 E_2)$, as quantified by (**a**) logarithmic negativity, (**b**) discord and (**c**) classical correlations as the system evolves according to Equation (24). Time is denoted t, and p determines the Werner state of the environment at $t = 0$. The system is initially in the vacuum state $|0\rangle$.

However, the growth in entanglement when $p \approx 0$ is quite surprising: S and the environment are more entangled when $p = 0$ than when such parameter takes a small ($\lesssim 0.2$) yet non-zero value, even though the environment has more quantum and classical correlations, initially, in this case. This could also relate to correlations of a nature that are different from entanglement. To address this, we use figures of merit for quantum and classical correlations defined as in Refs. [26,27]. First, we quantify classical correlations in a bipartite system composed of A and B using the generalized conditional entropy

$$J(A|B) = \max_{B_i^\dagger B_i} \left(S(\rho_A) - \sum_i p_i S(\rho_A^i) \right), \tag{27}$$

where $B_i^\dagger B_i$ is a POVM on system B, $\rho_A = \mathrm{Tr}_B[\rho_{AB}]$ and ρ_A^i is the state of ρ_A after system B has been measured with $B_i^\dagger B_i$. This enables us to find the maximum information we can gain about system A by measuring system B. As for quantum correlations, we resort to discord [28], namely the difference between total correlations (as measured by the quantum mutual information) and classical correlations

$$\mathcal{D}(A|B) = I(\rho_{AB}) - J(A|B). \tag{28}$$

For simplicity, the maximum entailed by the definition of $J(A|B)$ will be sought over all projective measurements only, following the examples in Refs. [29,30]. While this is accurate and rigorous only for two-qubit systems, for our three-qubit problem, we will only be able to quantify lower (upper) bounds to classical (quantum) correlations.

Starting from the same initial state of $|\psi\rangle_S = |0\rangle$, discord and classical correlations for the bipartition S-vs-$(E_1 E_2)$ are shown in Figure 5b,c, where we can appreciate a behavior that is, qualitatively, the inverse of entanglement: larger degrees of discord and mutual information are found in the state at hand as p decreases, which is somewhat counterintuitive. Therefore, while entanglement and non-Markovianity may be connected, we can conclude that discord and classical correlations are not linked to non-Markovianity.

It is important to note that at the end of the protocol (i.e., for $t = 1$), only classical system-environment correlations remain for $p < 1$. The information about $|\psi\rangle$ is encoded in such correlations, and thus, information back-flow is prevented. This is the reason behind the reduced success of the protocol as p diminishes.

As the initial state of the system directly affects how entanglement is shared during the protocol (as highlighted in Section 2), without affecting the performance of the protocol, we addressed the case of inputting state $|+\rangle$ rather than $|0\rangle$. However, the results were similar to all the same features visible in the behavior of each figure of merit of correlations.

As in Section 3.2, we now change the dynamics to that in Equation (25), and thus assume that each gate can be independently performed one by one. We begin, as before, with the initial system state $|\psi\rangle_S = |0\rangle$. The correlations are shown in Figure 6, which displays some similarities with the study performed in Figure 5. As in the previous case, the entanglement between S and $E_1 E_2$ is larger for larger p [cf. Figure 6a]. However, for this implementation of the quantum circuit operations, there is no unexpected growth in entanglement for $p \simeq 0$. Moreover, entanglement only appears when the final gate of the circuit is performed, which is precisely when the trace distance rises in Figure 3, signaling non-Markovianity. This all heavily implies that entanglement is necessary for non-Markovian dynamics in the protocol.
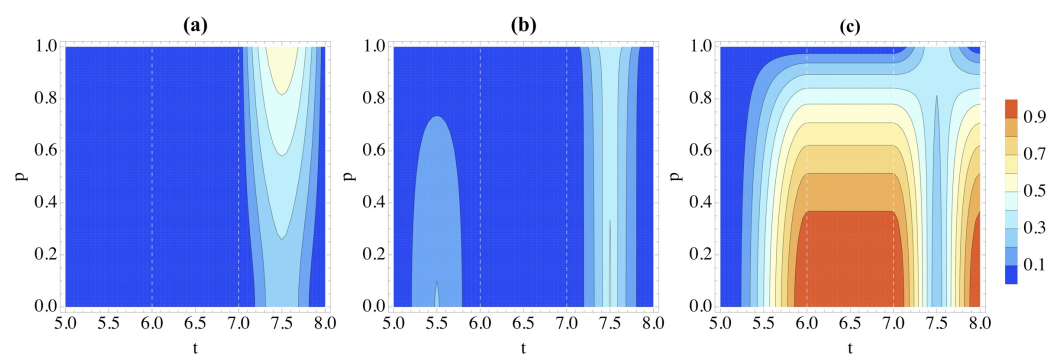

Figure 6. Correlations in the partition $S|E_1 E_2$ as quantified by (**a**) logarithmic negativity, (**b**) discord and (**c**) classical correlations when the Hamiltonian of the system and environment is given by Equation (25). We take the initial state of the system to be $|0\rangle$ and the environment $W(p)$. Here t is a dimensionless time. We only show $5 \leq t \leq 8$ as there are no system-environment correlations before $t = 5$.

The discord and classical correlations in Figure 6b,c also share features of those in Figure 5; they are both larger for smaller p. When $p = 1$, these correlations grow and vanish only during G_8, the SWAP gate between S and E_1. However, they can also appear during G_6 when $p < 1$.

At first glance, the two types of dynamics seem to result in similar dynamics. However, we see stark changes when we change the system's initial state. Although the features of the correlation dynamics remain much the same for the dynamics in Equation (24), they are remarkably different when we change the initial state from $|0\rangle$ to $|+\rangle$ when the Hamiltonian is that in Equation (25). This can be easily seen by comparing Figures 6 and 7. After the initial CNOT operation, the system and environment become entangled; this is reflected in both Figure 7a,b. This means that we now see more discord between S and $E_1 E_2$ for larger p rather than smaller; the opposite trend when the initial state is $|0\rangle$. However, entanglement is similar; the more entanglement, the more non-Markovianity. Now, we see a small spike during the final gate of the circuit, similar to the unusual resurgence of entanglement when $p = 0$ in the overlapping gates case.
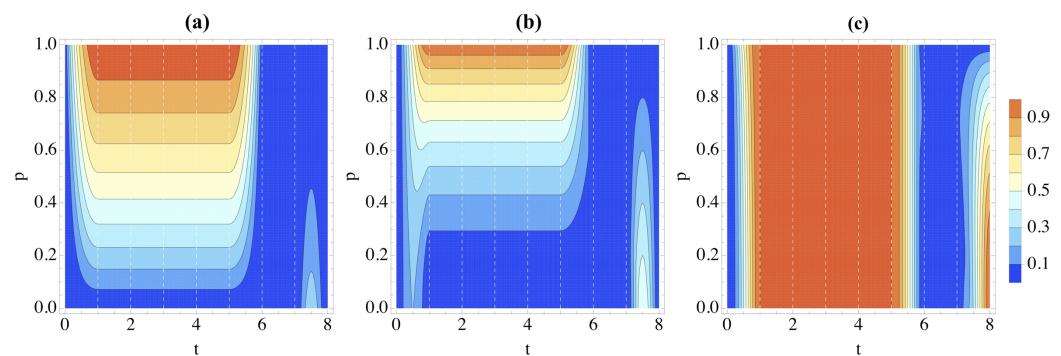
Figure 7. Correlations in the partition $S|E_1 E_2$ as quantified by (**a**) logarithmic negativity, (**b**) discord and (**c**) classical correlations when the Hamiltonian of the system and environment is given by Equation (25). We take the initial state of the system to be $|+\rangle$ and the environment $W(p)$.

5. Conclusions

We have critically addressed a measurement-free quantum teleportation protocol against the claim that non-Markovianity is needed to boost the teleportation performance [4]. We have shown that such a connection crucially depends on the way the operations entailed by the protocol are actually implemented. When chopping the circuit in individual gates acting on—in general multiple—elements of the register, a more definite relation between the performance of teleportation and non-Markovianity can be spotted, while the evidence of a key role played by non-Markovianity remains weak. On the one hand, the negative results reported here reinforce the need for a comprehensive and rigorous resource theory of non-Markovianity for quantum information processing (some interesting initial attempts at establishing such a theory have been made [18,19]). On the other hand, it emphasizes the relevance of the actual way a given quantum protocol is implemented in determining the quantities that are fundamental to its performance.

Author Contributions: Conceptualization, H.M. and M.P.; formal analysis, H.M. and M.P.; writing—original draft preparation, H.M.; writing—review and editing, M.P. All authors have read and agreed to the published version of the manuscript.

Data Availability Statement: The data presented in this study are available from the authors upon reasonable request.

Conflicts of Interest: The authors declare no conflicts of interest.

References

1. Bennett, C.H.; Brassard, G.; Crépeau, C.; Jozsa, R.; Peres, A.; Wootters, W.K. Teleporting an unknown quantum state via dual classical and Einstein-Podolsky-Rosen channels. *Phys. Rev. Lett.* **1993**, *70*, 1895. [CrossRef] [PubMed]
2. Briegel, H.J.; Browne, D.E.; Dür, W.; Raussendorf, R.; Van den Nest, M. Measurement-based quantum computation. *Nat. Phys.* **2009**, *5*, 19. [CrossRef]
3. Brassard, G.; Braunstein, S.L.; Cleve, R. Teleportation as a quantum computation. *Physica D* **1998**, *120*, 43. [CrossRef]
4. Tserkis, S.; Head-Marsden, K.; Narang, P. Information back-flow in quantum non-Markovian dynamics and its connection to teleportation. *arXiv* **2022**, arXiv:2203.00668. [CrossRef]
5. de Vega, I.; Alonso, D. Dynamics of non-Markovian open quantum systems. *Rev. Mod. Phys.* **2017**, *89*, 015001. [CrossRef]
6. Breuer, H.P.; Laine, E.M.; Piilo, J.; Vacchini, B. Colloquium: Non-Markovian dynamics in open quantum systems. *Rev. Mod. Phys.* **2016**, *88*, 021002. [CrossRef]
7. Rivas, A.; Huelga, S.F.; Plenio, M.B. Quantum non-Markovianity: Characterization, quantification and detection. *Rep. Prog. Phys.* **2014**, *77*, 094001. [CrossRef]

8. Laine, E.M.; Breuer, H.P.; Piilo, J. Nonlocal memory effects allow perfect teleportation with mixed states. *Sci. Rep.* **2014**, *4*, 4620. [CrossRef]

9. Liu, Z.D.; Sun, Y.N.; Liu, B.H.; Li, C.F.; Guo, G.C.; Hamedani Raja, S.; Lyyra, H.; Piilo, J. Experimental realization of high-fidelity teleportation via a non-Markovian open quantum system. *Phys. Rev. A* **2020**, *102*, 062208. [CrossRef]

10. Hesabi, S.; Afshar, D. Non-Markovianity measure of Gaussian channels based on fidelity of teleportation. *Phys. Lett. A* **2021**, *410*, 127482. [CrossRef]

11. Wang, Y.; Xue, S.; Song, H.; Jiang, M. Robust quantum teleportation via a non-Markovian channel. *Phys. Rev. A* **2023**, *108*, 062406. [CrossRef]

12. Bowen, G.; Bose, S. Teleportation as a Depolarizing Quantum Channel, Relative Entropy, and Classical Capacity. *Phys. Rev. Lett.* **2001**, *87*, 267901. [CrossRef] [PubMed]

13. Gu, Y.J.; Yao, C.M.; Zhou, Z.W.; Guo, G.C. General teleportation as a quantum channel. *J. Phys. A Math. Gen.* **2004**, *37*, 2447. [CrossRef]

14. Nielsen, M.A.; Caves, C.M. Reversible quantum operations and their application to teleportation. *Phys. Rev. A* **1997**, *55*, 2547. [CrossRef]

15. Pirandola, S.; Laurenza, R.; Ottaviani, C.; Banchi, L. Fundamental limits of repeaterless quantum communications. *Nat. Commun.* **2017**, *8*, 15043. [CrossRef]

16. Pirandola, S.; Braunstein, S.L.; Laurenza, R.; Ottaviani, C.; Cope, T.P.W.; Spedalieri, G.; Banchi, L. Theory of channel simulation and bounds for private communication. *Quantum Sci. Technol.* **2018**, *3*, 035009. [CrossRef]

17. Tserkis, S.; Dias, J.; Ralph, T.C. Simulation of Gaussian channels via teleportation and error correction of Gaussian states. *Phys. Rev. A* **2018**, *98*, 052335. [CrossRef]

18. Berk, G.D.; Garner, A.J.P.; Yadin, B.; Modi, K.; Pollock, F.A. Resource theories of multi-time processes: A window into quantum non-Markovianity. *Quantum* **2021**, *5*, 435. [CrossRef]

19. Bhattacharya, S.; Bhattacharya, B.; Majumdar, A.S. Convex resource theory of non-Markovianity. *J. Phys. A Math. Theor.* **2021**, *54*, 035302. [CrossRef]

20. Breuer, H.P.; Laine, E.M.; Piilo, J. Measure for the degree of non-Markovian behavior of quantum processes in open systems. *Phys. Rev. Lett.* **2009**, *103*, 210401. [CrossRef]

21. Wißmann, S.; Karlsson, A.; Laine, E.M.; Piilo, J.; Breuer, H.P. Optimal state pairs for non-Markovian quantum dynamics. *Phys. Rev. A* **2012**, *86*, 062108. [CrossRef]

22. Rivas, A.; Huelga, S.F.; Plenio, M.B. Entanglement and non-Markovianity of quantum evolutions. *Phys. Rev. Lett.* **2010**, *105*, 050403. [CrossRef] [PubMed]

23. Luo, S.; Fu, S.; Song, H. Quantifying non-Markovianity via correlations. *Phys. Rev. A* **2012**, *86*, 044101. [CrossRef]

24. Plenio, M.B. Logarithmic Negativity: A Full Entanglement Monotone That is not Convex. *Phys. Rev. Lett.* **2005**, *95*, 090503. [CrossRef]

25. Horodecki, R.; Horodecki, P.; Horodecki, M.; Horodecki, K. Quantum entanglement. *Rev. Mod. Phys.* **2009**, *81*, 865–942. [CrossRef]

26. Ollivier, H.; Zurek, W.H. Quantum discord: A measure of the quantumness of correlations. *Phys. Rev. Lett.* **2001**, *88*, 017901. [CrossRef]

27. Henderson, L.; Vedral, V. Classical, quantum and total correlations. *J. Phys. A Math. Gen.* **2001**, *34*, 6899. [CrossRef]

28. Modi, K.; Brodutch, A.; Cable, H.; Paterek, T.; Vedral, V. The classical-quantum boundary for correlations: Discord and related measures. *Rev. Mod. Phys.* **2012**, *84*, 1655–1707. [CrossRef]

29. Galve, F.; Giorgi, G.L.; Zambrini, R. Orthogonal measurements are almost sufficient for quantum discord of two qubits. *Europhys. Lett.* **2011**, *96*, 40005. [CrossRef]

30. Al-Qasimi, A.; James, D.F.V. Comparison of the attempts of quantum discord and quantum entanglement to capture quantum correlations. *Phys. Rev. A* **2011**, *83*, 032101. [CrossRef]